CAL-2151

National Aeronautics and Space Administration

High-Energy Astrophysics Theory & Data Analysis Program

ANNUAL STATUS REPORT FOR NAGW-3075

Submitted to:

Dr. Louis J. Kaluzienski (Code SZC)
Technical Officer for NAGW-3075
National Aeronautics and Space Administration
300 E. Street, SW
Washington, DC 20546

Prepared by:

Columbia Astrophysics Laboratory
Departments of Astronomy and Physics
Columbia University
538 West 120^{th} Street
New York, New York 10027

Submitted by:

The Trustees of Columbia University
in the City of New York
Box 20, Low Memorial Library
New York, NY 10027

Title of Research:

High-Energy Astrophysics: A Theoretical Analysis of Thermal Radiation from Neutron Stars

Principal Investigator:

James H. Applegate
Columbia University

Report Period:

1 April 1993 – 31 March 1994

January 1994

SECOND ANNUAL REPORT FOR GRANT NAGW-3075

A THEORETICAL ANALYSIS OF THERMAL RADIATION FROM NEUTRON STARS

James H. Applegate

Department of Astronomy, Columbia University

538 West 120th Street, New York, NY 10027

INTRODUCTION

This report describes work completed or in progress during the second year of the three year grant NAGW-3075, A Theoretical Analysis of Thermal Radiation Form Neutron Stars, to Principal Investigator James H. Applegate. The bulk of the grant funds go to the partial support of a postdoc, Dr. Dany Page. The work described below is a substantial portion of Dr. Page's research activities fro the past year. This work was carried out under the supervision of Dr. Applegate.

WORK COMPLETED

The unambiguous detection of thermal radiation from the surface of a cooling neutron star was one of the most anxiously awaited results in neutron star physics. This particular Holy Grail was found by Halpern & Holt (1992), who used ROSAT to detect pulsed X-rays from the γ-ray source Geminga and demonstrate that it was a neutron star, probably a radio pulsar beamed away from us. Two other pulsars, PSR 0656+14 (Finley, Ogelman, & Kiziloğlu 1992) and PSR 1055-52 (Ogelman & Finley 1993), have also been detected in thermal X-rays by ROSAT. These results caused us to turn our attention away from developing ever more sophisticated cooling codes to applying our models to understand the new data.

At an age of $\sim 3.4 \times 10^5$years, Geminga is in the photon cooling era. We have shown that its surface temperature of 5.2×10^5K can be explained within the contexts of both the slow (modified Urca only in the interior) and fast (direct Urca, pions, kaons, etc) cooling scenarios; Geminga is too old to distinguish between these possibilities. However, agreement between the predictions and observations in either scenario is only possible if baryons are paired (BCS pairing, as in superconductors) within most, if not all, of the interior of the star. In the slow cooling scenario, the surface temperature is too high unless the specific heat of the interior is reduced by extensive baryon pairing. In the fast

cooling scenario, the surface temperature will be much too low unless the fast neutrino cooling is shut off by baryon pairing (see Page & Applegate 1992). In this case the pairing must extend throughout the entire interior, and involve every particle species that can participate in fast cooling. These results are the strongest case to date for the necessity of baryon pairing in the interior of a neutron star; neutron pairing in the inner crust is an essential ingredient in the vortex line depinning theory of pulsar glitches, but this theory makes no statements about the baryons in the interior of the star.

We also comment on the surface temperature determinations for the pulsars PSR 0656+14 and PSR 1055-52, both of which are also in the photon cooling era. If the fast cooling scenario is correct, these stars also require baryon pairing throughout their cores. However, the observational uncertainties are larger for these pulsars than for Geminga, and a very conservative interpretation of the data using slow cooling and no pairing is allowed.

This work has been written up and is accepted for publication in The Astrophyscial Journal (Page 1994). Preliminary versions have already appeared (Page 1993a,b).

WORK IN PROGRESS

All of our neutron star cooling models to date have used the unmagnetized effective temperature-interior temperature relation for the outer boundary condition. We are improving the models by using published magnetic envelope calculations and assumed geometried for the surface magnetic field to determine local interior temperature-emitted flux relations for the surface of the star. The magnetic field makes the electron contribution to the thermal conductivity (the most important factor in determining the interior temperature-emitted flux relation) highly anisotropic; heat flows much more easily along the field lines than across them. As a result, regions of the surface where the magnetic field is nearly normal to the surface will be hotter than average and regions where the field

is nearly tangential will be colder than average. Our procedure will allow us to include the effect of these temperature variations in our light curves.

The four neutron stars for which there is good evidence that ROSAT has detected thermal emission from the surface (Vela, Geminga, 1055-52, and 0656+14) all have pulse fractions between 10% and 20% in the 0.08-0.50 keV band, which is the energy band most sensitive to thermal emission. From the work done so far, we conclude that there must be large temperature differences on the surface to account for these pulse fractions. These pulse fractions may provide interesting information about the configuration of the surface magnetic field of the neutron star. For example, models with a simple dipole field cannot produce pulse fractions as large as observed if the variation in surface temperature is entirely due to anisotropic thermal conduction.

We have used blackbody emission at the local surface temperature for the emergent spectrum in our calculations. We hope to drop this approximation in favor of spectra of magnetic atmospheres in the future, although this undertaking may be beyond the scope of the current three year project due to its complexity.

REFERENCES

Halpern, J.P. & Holt, S.S. 1992 Nature, 357, 222.

Finley, J.P., Ogelman, H., & Kiziloglu, U. 1992 ApJ, 394, L21.

Ogelman, H. & Finley, J.P. 1993 ApJ, 413, L31.

Page, D. & Applegate, J.H. 1992 ApJ, 394, L17.

Page, D. 1993a in Proceedings of the First Symposium on Nuclear Physics in the Universe, ed. M.R. Strayer & M.W. Guidry, Bristol: Adam Hilger & Co..

Page, D. 1993b in Lives of the Neutron StarsNATO Advanced Study Institute, Kemer, Turkey, Aug. 29 -Sept. 11, 1993.

Page, D. 1994 to appear in ApJ June 10, 1994.

Poster presented at the NATO ASI 'LIVES of the NEUTRON STARS'
Kemer, Turkey, Aug. 29 - Sept 11, 1993

SURFACE TEMPERATURE OF A MAGNETIZED NEUTRON STAR: LIGHT CURVES AND SPECTRA FOR GEMINGA

Dany Page
Department of Astronomy, Columbia University
Instituto de Astronomía, Universidad Nacional Autónoma de México

1. INTRODUCTION

The high quality ROSAT data from the nearby neutron stars Vela, PSR 0646+14, Geminga and PSR 1055-52 present a new chalenge for theorists to provide good models for their interpretation. The published preliminary analyses of these data have shown that a large part of the soft X-ray received by ROSAT most probably come from the neutron star surface (in the case of Vela the contribution of the surrounding synchroton nebula has to be first separated).

The strong magnetic field present at the neutron star surface affects the characteristics of the emitted radiation, significantly changing the spectrum as discussed by Pavlov and Shibanov in this workshop. Some of the resulting magnetized spectra have been used in data analyses and have led to substantially different conclusions about the neutron star surface temperature when compared with analyses using simple black body spectra. All these works have so far assumed a uniform temperature distribution on the neutron star surface, with the exception of the inclusion of the contribution of the hot polar caps. However, another important effect of the magnetic field is to introduce a strong anisotropy of the heat transport in the outermost layers below the photosphere, resulting in a non-uniform surface temperature distribution.

We present here some preliminary results of our modelling of this non-uniform surface temperature distribution. Beside generating composite spectra (from the temperature distribution) and phase dependent spectra (from the star's rotation) we also naturally have the capability to produce light curves, thus adding a new dimension to the interpretation of the data. The prospect of this approach is not only to obtain more reliable measurements of neutron star surface temperatures, but also to learn about the configuration of the surface magnetic field. Our results so far use local black body emission; we hope to use more realistic spectra in the future.

2. SURFACE TEMPERATURE

All neutron stars of interest have an isothermal interior surrounded by an envelope where a strong temperature gradient is present. Isothermality is reached at densities lower than $10^{10} gm/cm^3$, corresponding to a depth of at most 100 meters. Gundmundsson *et al.* (1983) have shown that the relationship between the interior temerature T_i and the uniform surface temperature T_s in absence of a magnetic field is

$$T_{s,6} \sim T_{i,8}^{1/2} \tag{1}$$

($T_n = T/10^n K$). This relation is mostly determined by the electron conductivity at densities ranging from $\sim 10^4$ to $10^8 gm/cm^3$ depending on the surface temperature. In presence of a strong magnetic field $\mathbf{H}$ the electrons are still free to move parallelly to $\mathbf{H}$ but their motion in the perpendicular directions is strongly inhibited. Detailed calculations have shown that the electron thermal conductivity is slightly increased along the field and strongly suppressed perpendicularly to the field. Compared to the zero field result, for a given internal temperature, the surface temperature will be slightly higher in regions where the field is almost radial but much lower in regions where the field is tangent to the surface.

Due to the thinness of the layer where the magnetic effects are important the heat transport is still a one dimensional problem, at least in a first approximation. For a given surface magnetic field configuration $\mathbf{H}(\theta, \phi)$ the surface temperature $T_s(\theta, \phi)$ depends only on the angle Θ between the normal $\mathbf{n}$ and $\mathbf{H}$ as well as the internal uniform temperature T_i

$$T_s(\theta, \phi) = T_s(\Theta, T_i) \tag{2}$$

For parallel transport, $\Theta = 0$, we use the results of Hernquist (1985) and for orthogonal transport, $\Theta = 90^0$, we use Schaaf (1990a). For an arbitrary Θ Schaaf (1990b) has presented a two dimensional calculation and written his results in the form

$$T_s(\Theta) = \xi(\Theta) \times T_s(\Theta = 0) \tag{3}$$

where

$$\xi(\Theta) = \xi_0 + (1 - \xi_0) \cos(\Theta)^\alpha. \tag{4}$$

Thus $\xi(\Theta = 0) = 1$ and $\xi_0 = T_s(\Theta = 90^0)/T_s(\Theta = 0) \leq 1$. The exponent $\alpha \sim 1$ is itself a weak function of $\mathbf{H}$ and T_i.

3. GENERATING SPECTRA AND LIGHT CURVES

Th procedure we use is as follows:

- Choose the star's mass M and radius R.
- Choose a surface magnetic field configuration $\mathbf{H}(\theta, \phi)$. So far we have only considered dipolar fields but more general configurations can easily be incorporated.
- Choose the internal temperature T_i. With this we generate the surface temperature distribution $T_s(\theta, \phi)$ as described in Section 2 (see Figure 1).
- Choose the observer's position, i.e. the angle α between the rotation axis and the observer direction.
- Rotate the star. We take 60 positions and at each position take a snap-shot of the star: we integrate the emitted flux over the visible part of the surface, taking into account gravitational lensing. This produces 60 phase dependent spectra which are then red-shifted.
- Choose the star's distance D and the column density N_H for interstellar absorption to obtain the phase dependent spectra as received at the entrance of the ROSAT telescope.
- The spectra are passed through the PSPC resolution matrix to obtain the time (= phase) dependent predicted count rates.

At each point of the star's surface we use **black body emission** at the corresponding temperature. Our spectra are thus composite black body spectra. We hope to consider more realistic magnetic spectra in the future.

4. PRELIMINARY RESULTS FOR GEMINGA

We borrow the basic characteristics of our analysis from the study of Halpern & Ruderman (1993, referred to as HR bellow), who considered both X-ray data from ROSAT and γ-ray data from GRO. The results we are presenting here have to be considered as illustrative: the number of degrees of freedom in our model is so large that we have not yet been able to do a comprehensive study. Moreover our method still uses local black body spectra.

Beside the surface temperature distribution we also include two polar caps of adjustable size and temperature, located at the points where the magnetic dipole axis crosses the star's surface. Within the restricted parameter search we have done, the configuration which gave the best fit to the published Geminga data (HR) is the following (see figures):

- $M = 1.4 M_\odot$ and $R = 12\ km$ (giving $R^\infty = 14.8\ km$). No search was done on these two parameters, we just use typical values. The red-shift factor is $e^\phi = 0.8$ and the maximum lensing angle $\theta_{max} = 120.7^0$ (instead of 90^0 in flat space-time).

- Off-center surface magnetic dipole field, in the equatorial plane (from HR: casi orthogonality of the dipole with the rotation axis is required by the γ-ray data within the outer-gap model; off-centering is needed to obtain a single peak in the upper energy X-ray light-curve).
  The center of the dipole is 2.4 km away from the star's center and at an angle of 60^0 with the radius (from fitting of the lower energy X-ray light-curve: distance from the center is restricted by the amplitude of light-curve, orientation with respect to the radius is used to reproduce the slight skewness of the light-curve)

- Internal temperature $T_i = 4 \times 10^7 K$ (from fitting of the lower energy spectrum), giving en effective temperature at infinity $T^\infty_{eff} = 4.47 \times 10^5 K$ and an average temperature (at infinity) $T^\infty_{ave} = 4.18 \times 10^5 K$. The maximum and minimum surface temperatures are respectively $T^\infty_{max} = 5.36 \times 10^5 K$ and $T^\infty_{min} = 1.20 \times 10^5 K$.

- Two polar caps of diameter 0.44 degree and temperature $T^\infty_{cap} = 3.2 \times 10^6 K$ (HR: from fitting of the upper energy component of the spectrum).

- Distance $D = 120\ pc$ and column density $N_H = 3.8 \times 10^{20}\ cm^{-2}$ (from fitting of the lower energy spectrum).

As can be seen from the figures 2 and 3 the fit of the lower energy light-curve is quite good as well as the fit to the spectrum.

5. COMMENTS

From the figures and experiences from the other trials we have done we can make the following comments:

1. The light curves are quite smooth (of course), and gravitational lensing can only make them smoother. The sharp dips that seem to be present particularly in the lower energy curve could be **evidence for some magnetospheric absorption.**

2. HR argued that the relative flatness of the medium energy light curve could come from a compensation between the lower and upper energy curves which are about 105^0 out of phase. If the upper energy curve is interpreted as thermal emission from the two hot polar caps then the contribution of these caps to the medium energy curve is totally negligeable: the flatness of this light curve must be explained by another mechanim. **Anisotropic emission due to the magnetic field effects** could be such a mechanims.

3. With all surface *dipolar* magnetic field configurations we have tried it was impossible to obtain a shift between the maxima of the lower energy light curve (due to emission from the main surface) and the upper energy light curve (due to polar cap emission): this could be an **argument against a dipolar surface field** (in case anybody needs such an argument).

4. The PSPC resolution matrix we use is a more recent version than the one used by HR. It seems that the spectral fits need lower temperatures than in HR and also larger column densities. The value of $N_H = 3.8 \times 10^{20}\ cm^{-2}$ used in the figures is *much too large* for a distance of 120 pc. If this is confirmed, it would be a strong argument for the **inadequacy of the black body emission.** A H or He atmosphere spectrum with low interstellar absorption should give results similar to a black body spectrum with strong interstellar absorption (but with a different temperature and star's distance).

REFERENCES

Gudmundsson E. H., Pethick C. J. & Epstein R. I., 1983, Ap.J. **272** p.286.
Halpern J. P. & Ruderman M., 1993, submitted to Ap.J.
Hernquist L., 1985, MNRAS **213** p.313.
Schaaf M. E., 1990a, A&A **227** p. 61.
Schaaf M. E., 1990b, A&A **235** p. 499.

FIGURE 1. Temperature distribution on the star's surface, area preserving projection. The values indicated along the isocurves are local temperatures, non red-shifted. The surface magnetic field is dipolar, in the equatorial plane, 20% off center and it makes an angle of 60^0 with the radius. One hemisphere is warmer than the other, producing the skewness of the light curve in Fig. 3.

FIGURE 2. Observed and theoretical spectra, in the ROSAT PSPC detector. The data are from Halpern & Ruderman (1993). The surface temperature distribution is shown in Fig. 1 and the observer is in the equatorial plane, at a distance of 120 pc ($N_H = 3.8 \times 10^{20}$ cm^{-2}). The upper energy component (E > 0.5 keV) comes from the two hot polar caps ($T_{cap} = 4 \times 10^6$ K). The separate contributions from the main surface and the polar caps are shown as dashed lines. These results are similar to the results of Halpern & Ruderman (1993). The dash-dot line is a black body at the effective temperature $T_{eff} = 5.6 \times 10^5$ K and the dash-triple dot curve is a black body at the average temperature $T_{ave} = 5.23 \times 10^5$ K (non red-shifted values).

FIGURE 3. Observed and theoretical light curves, in the ROSAT PSPC detector. The data are from Halpern & Ruderman (1993). The continuous curves are the total emission, main surface + polar caps, while the dotted curves show the contribution from the main surface only. Notice that in the middle energy range the contribution from the polar caps is negligeable. In the upper energy band the contributions from each polar cap are shown as dash-dot and dash-tripple dot curves.

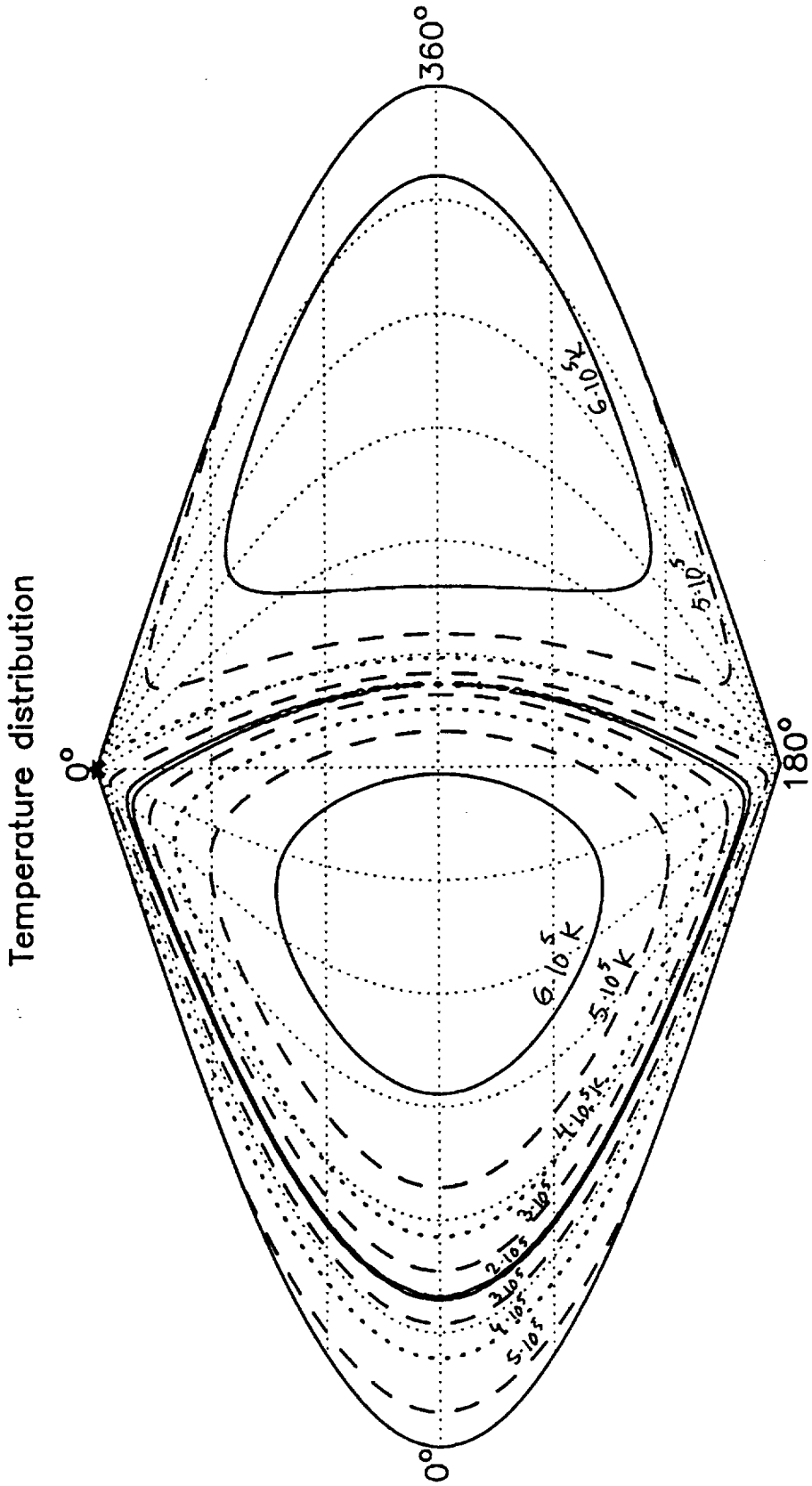
Temperature distribution
360°
0°
180°
0°
6.10⁵K
5.10⁵K
4.10⁵K
3.10⁵
2.10⁵
3.10⁵
4.10⁵
5.10⁵

Figure 1.

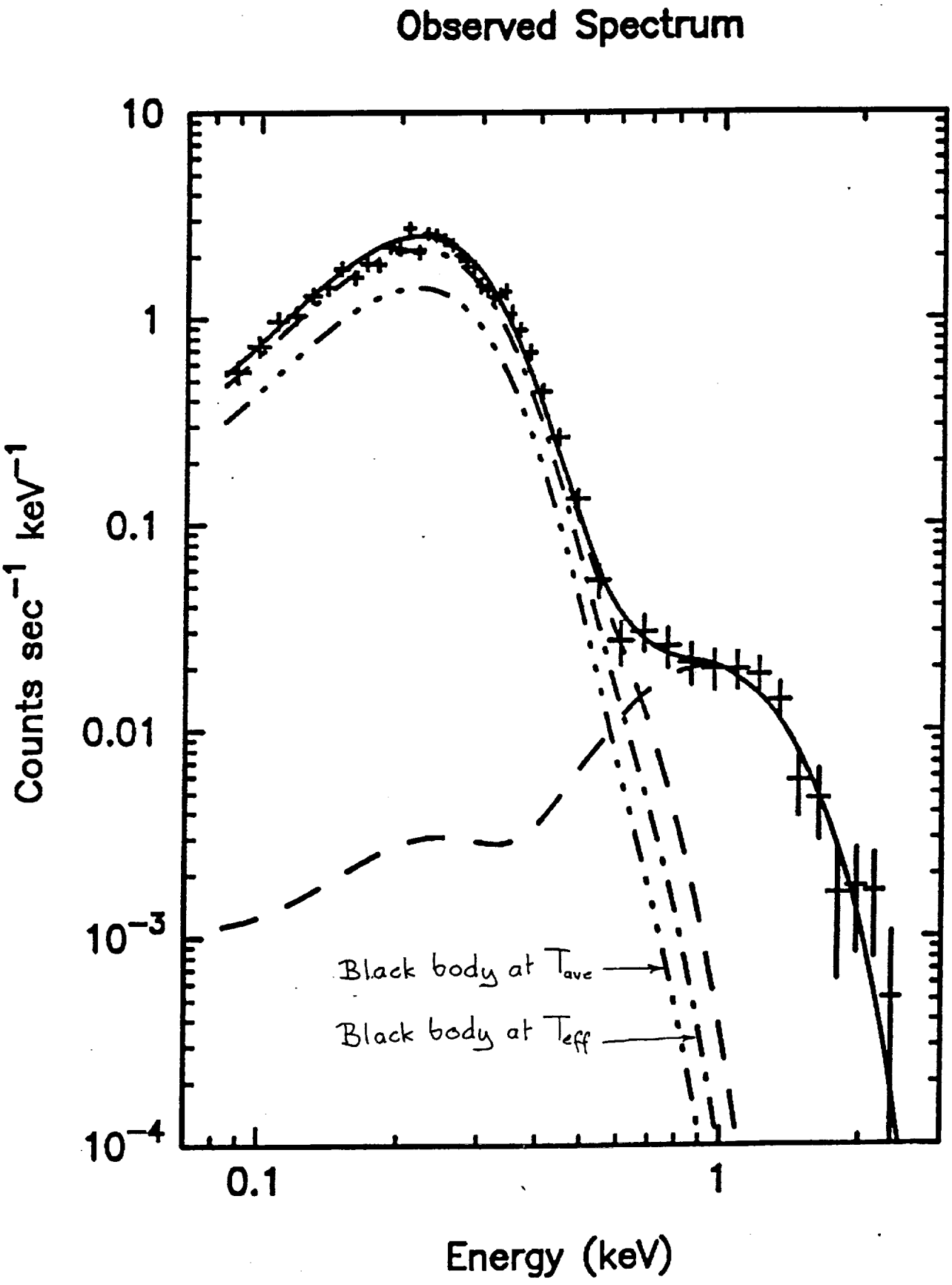
Observed Spectrum
10
1
0.1
0.01
10^{-3}
10^{-4}
Counts sec^{-1} keV^{-1}
0.1
1
Energy (keV)
Black body at T_{ave}
Black body at T_{eff}

Figure 2

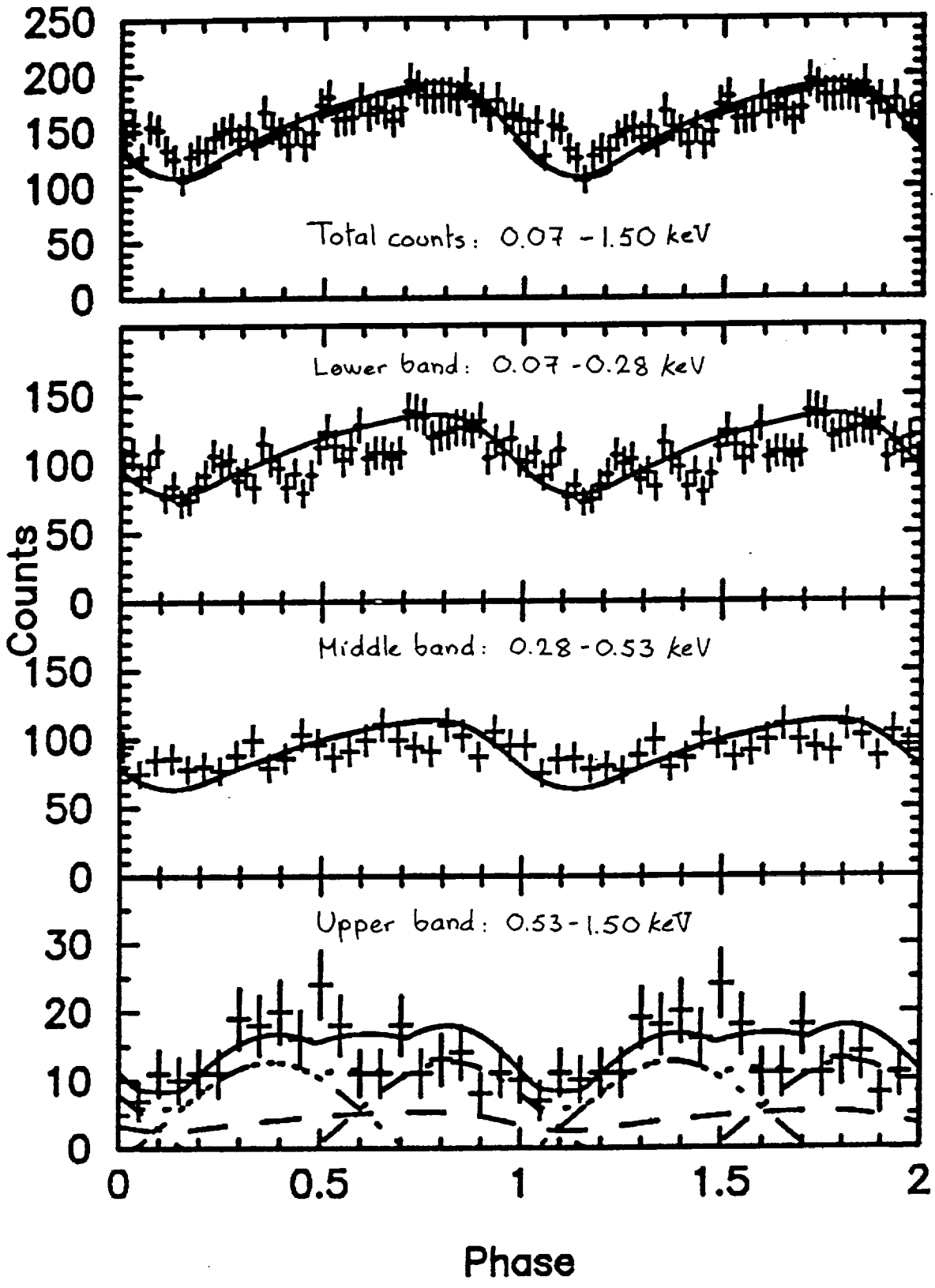
Light Curves
Total counts: 0.07 - 1.50 keV
Lower band: 0.07 - 0.28 keV
Middle band: 0.28 - 0.53 keV
Upper band: 0.53 - 1.50 keV
Counts
Phase
250
200
150
100
50
0
150
100
50
0
150
100
50
0
30
20
10
0
0
0.5
1
1.5
2

Figure 3.

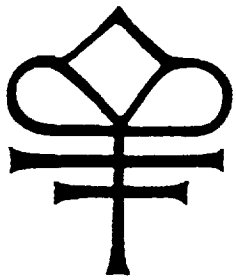

GEMINGA : A COOLING SUPERFLUID NEUTRON STAR

Dany Page

Department of Astronomy, Columbia University
538 West 120th Street, New York, NY 10027

Submitted to *The Astrophysical Journal*

COLUMBIA UNIVERSITY

DEPARTMENTS OF

PHYSICS and ASTRONOMY

NEW YORK, NEW YORK 10027

GEMINGA :
A COOLING SUPERFLUID NEUTRON STAR

Dany Page

Department of Astronomy, Columbia University

538 West 120th Street, New York, NY 10027

ABSTRACT

We compare the recent temperature estimate of Geminga with neutron star cooling models. Due to its age ($\sim 3.4 \times 10^5$ years) Geminga is in the photon cooling era and it is shown that its surface temperature ($\sim 5.2 \times 10^5$ K) can be understood by both types of neutrino cooling scenarios, i.e slow neutrino cooling by the modified Urca process or fast neutrino cooling by the direct Urca process or some exotic matter, and thus does not allow to discriminate between these two competing schemes. However for both types scenarios agreement with the observed temperature can only be obtained if *baryon pairing is present in most, if not all, of the core of the star*. Within the slow neutrino cooling scenario the early neutrino cooling is not sufficient to explain the observed low temperature and extensive pairing in the core is necessary to reduce the specific heat and increase the cooling rate in the present photon cooling era. Within all the fast neutrino cooling scenarios pairing is necessary throughout the whole core to control the enormous early neutrino emission which, without pairing suppression, would result in a surface temperature at present time much lower than observed.

We also comment on the recent temperature estimates of PSR 0656+14 and PSR 1055-52 which pertain to the same photon cooling era. If one assumes that all neutron star undergo fast neutrino cooling then these two objects also provide evidence for extensive baryon pairing in their core, but observational uncertainties also permit a more conservative interpretation with slow neutrino emission and no pairing at all. We argue though that the observational evidence for the slow neutrino cooling model ('standard model') is in fact very dim and that the interpretation of the surface temperature of all neutron stars could be done with a reasonable theoretical *a priori* within the fast neutrino cooling scenarios only. In this case Geminga, PSR 0656+14 and PSR 1055-52 all show evidence of baryon pairing down to their very centers.

subject headings: dense matter — stars: neutron — stars: x-rays

1. INTRODUCTION

The study of the thermal evolution of young neutron stars offers the possibility to obtain unique information about the structure of compressed cold nuclear matter. The early cooling after the supernova explosion is driven by neutrino emission, whose rate is a very sensitive function of the state of that matter. Moreover, both the neutrino and the later photon coolings are strongly affected by the occurence of pairing (*à la* BCS) of the baryonic components of the star's core. These two aspects combined result in a wide range of predicted surface temperatures and give us two handles to extract information about the composition and pairing state of dense matter through comparison of neutron star cooling calculations with observations of neutron stars of known ages.

Observational candidates for this purpose must have an age well below 10^6 years since after this the star has exhausted its initial heat content and its (much lower) temperature depends on other mechanisms. Interstellar absorption is significant at the photon energies corresponding to the expected surface temperatures, of the order of 10^6 K or lower, and hence the star must be not too far away from us and in a region of low interstellar absorption. Until recently only three neutron stars fullfilled these two criteria of relative youth and closeness, all three located within the local bubble of low interstellar matter density surrounding the sun: PSR 0833-45 (Vela), PSR 0656+14 and PSR 1055-52, and provided the only reliable data to compare with theoretical models. Some other objects, as for exemple PSR 0531+21 (Crab; Harnden & Seward 1984) or the neutron star in the supernova remnant 3C58 (Becker, Helfand & Szymkowiak 1982), located at further distances have only given rough upper limits of their surface temperatures. We refer to Ögelman (1991) for a review of the pre-

ROSAT observational situation.

With the recent demonstration by Halpern & Holt (1992) that Geminga *is* a neutron star a new candidate is now available. The quality of the ROSAT data makes it one of the best cases of detection of thermal radiation from a neutron star surface to date, and the data analysis (Halpern & Ruderman 1993) is the most detailed performed so far. Geminga is one of the closest neutron stars and is located within the local interstellar bubble; Gehrels & Chen (1993) recently argued that the Geminga supernova may have actually been the cause of this bubble.

Comparison of the Geminga age and temperature with published models of neutron star cooling shows that the data can be accomodated by a variety of models. Several of the direct Urca cooling scenarios of Page & Applegate (1992), the kaon condensate cooling scenario of Page & Baron (1990) and some of the pion condensate cooling scenarios of Umeda *et al.* (1993b) work, while none of the fast cooling models, either with quarks or pion condensate, of Van Riper (1991) is successful. Some, but not all, of the 'standard' cooling models presented by Nomoto & Tsuruta (1986, 1987), Shibazaki & Lamb (1989), Page & Baron (1990), Van Riper (1991), Page & Applegate (1992) and Umeda *et al.* (1993a,b) are also successful. In this paper we will look at the various ingredients of these models and determine which ones are crucial for compatibility with this new neutron star. A preliminary version of this work has been presented in Page (1992).

The pulsars PSR 0656+14 and PSR 1055-52 have ages similar to Geminga and fit into the study of the present work. Since the analyses of the ROSAT observations of these two objects have been published recently (Finley, Ögelman & Kiziloğlu 1992 and Ögelman & Finley 1993) we will also discuss them briefly.

The structure of the paper is as follow. Section 2 presents the observational data

on Geminga. Section 3 describes the general physics of neutron star cooling relevent to our present purpose. Section 4 discusses the various fast neutrino cooling scenarios and section 5 presents detailed calculations within the slow neutrino cooling scenario. Comparison with Geminga is done in sections 4 and 5 while section 6 comments on the relevence of the previous results for other pulsars, in particular PSR 0656+14 and PSR 1055-52. Section 7 contains our conclusions.

2. GEMINGA

2.1 Geminga's age.

The Geminga period as measured by Halpern & Holt (1992) is $P = 0.2370974\ s \pm 0.1\mu s$. The earlier observation by COS-B and later GRO have slightly different P's which lie very accurately on a straight line (Bignami & Caraveo 1992) and give a practically constant period derivative of $\dot{P} = 1.099 \pm 0.001 \times 10^{-14}\ s\ s^{-1}$ over a span of 16 years. The corresponding spin-down age is $\tau = P/2\dot{P} = 3.4 \times 10^5$ years. This age is obtained with a braking index $n = 3$, i.e. with magnetic dipole braking. We will consider a range of ages corresponding to braking indices $n = 2$ and 4,

$$2.3 \times 10^5 \text{yrs} \leq t \leq 6.8 \times 10^5 \text{yrs}, \qquad (1)$$

the upper value being probably an overestimate. We refer to Michel (1991) and Lyne & Graham-Smith (1990) for a discussion of the reliability of the spin-down age as an indicator of the true age.

2.2 Geminga's temperature.

In the first estimate of the star's temperature Halpern & Holt (1992) fitted the two apparent components of the spectrum with a black body and a power law. The best fit gave a blackbody temperature of $T = 3-4 \times 10^5$ K. In a second more detailed analysis Halpern and Ruderman (1993) replaced the power law component by a second black body with higher temperature and argued that this hotter component ($T \cong 3 \times 10^6$ K) is due to emission from a reheated polar cap (this temperature is too high to be explained only by the anisotropy of heat transport in presence of a magnetic field). They obtained for the main surface emission a temperature $T = (5.2 \pm 1.0) \times 10^5$ K. From the ratio of the luminosities of these two components they concluded that the ratio of the areas of the hot and cold emitting regions is about 3×10^{-5}. Moreover it is likely that the surface is not emitting uniformly and that some colder region is not been seen, making the concept of 'surface temperature' an ambiguous one. However cooling calculations give as an output the effective temperature, i.e. a total luminosity, and the presence of a cooler region would reduce the luminosity and make the effective temperature somewhat lower than the inferred value of $(5.2 \pm 1.0) \times 10^5$ K.

All these analyses use black-body spectra but the surface of a neutron star cannot be expected to be a perfect black body. Romani (1987) has calculated more realistic spectra for various surface chemical compositions without magnetic field. Miller (1992) and Shibanov *et al.* (1992) have partially extended these results including the magnetic field effects. The general trend of these results, for H or He atmospheres, is that there is an excess emission in the Wien tail of the spectrum, compared to a blackbody, and the excess falls within the EINSTEIN and ROSAT detector ranges.

This excess is reduced if metals are present (due to absorption edges) or when the effects of the magnetic field are taken into account. As a consequence, the use of these spectra would lower the measured temperature. Finally some contamination from a surrounding nebula and/or surface reheating by gamma-rays or particles from the magnetosphere cannot be excluded. We refer to Halpern & Ruderman (1993) for a discussion.

We will take for comparison with our calculations an effective temperature of

$$4 \times 10^5 \mathrm{K} \leq T_e \leq 6 \times 10^5 \mathrm{K} \qquad (2)$$

but insist that it has to be taken as an upper limit for the above mentioned reasons. Being determined from the spectrum this temperature is independent of the distance, mass and radius of the star and is the 'temperature at infinity' T^∞, i.e. the red-shifted temperature.

3. PHYSICS OF NEUTRON STAR COOLING

At an age of a few times 10^5 years *Geminga is well into the isothermal phase* (Nomoto & Tsuruta 1987); its internal temperature T_i is uniform except for a gradient in the *envelope* just below the surface. The thermal evolution of the star is determined by energy conservation,

$$\frac{dE}{dt} = C_v \frac{dT_i}{dt} = -L_\nu - L_\gamma \qquad (3)$$

where E is the total thermal energy of the star, C_v its total specific heat, and L_ν and L_γ the total neutrino and photon luminosities (general relativistic correction factors are omitted here but were included in our calculations). The photon luminosity

is $L_\gamma = 4\pi R^2 \sigma T_e^4 \propto T_i^{2.2}$, where the effective temperature T_e is converted into an internal temperature T_i with the $T_i - T_e$ relationship calculated by Gudmundsson, Pethick & Epstein (1982,1983). The neutrino emissivities are proportional to T_i^6 or T_i^8 (see Table 1), hence photon emission from the surface will eventually dominate over neutrino emission when the temperature has dropped sufficiently. This turnover happens before the star reaches 10^5 years : *Geminga is thus well into the photon cooling era.* In this phase the cooling rate is mostly determined by the total specific heat of star but the actual surface temperature also depends on the previous neutrino cooling which can be considered as giving the initial condition for photon cooling.

Our cooling curves are calculated with the Heyney-type code already presented in Page & Baron (1990) and Page & Applegate (1992) which solves the general relativistic heat transport and energy balance equations. We refer to these papers for more details.

3.1 Neutrino processes.

The dominant neutrino emission processes occur in the core of the star and are variants of beta and inverse beta decay. Table 1 shows the approximate emissivities of several processes for comparison. One can divide them into slow and fast neutrino emission, depending if they involve four or two baryons. The large difference between slow and fast processes comes mainly from phase space considerations: Fermi's Golden Rule tells us that the rate is proportional to the total phase space volume available for both initial and final particles, and for fermions this volume is proportional to $k_B T/E_F$ where E_F is the particle Fermi energy. Typical nucleon Fermi energies in neutron star cores are of the order of a few tens to a few hundreds of MeV; if one take a typical temperature of $T = 10^9 \mathrm{K} \cong 0.1 \mathrm{MeV}/k_B$ and $E_F \sim 10^2$ MeV then a four

fermion process is about $(k_B T/E_F)^2 \sim 10^{-6}$ time weaker than a two fermion process, which is what the direct Urca - modified Urca emissivities show. Participation of a meson (pion or kaon) in a process does not introduce any phase space limitation since these are bosons, but strong interactions effects, and strangeness violation in the case of kaons, reduce their efficiency compared to the simple direct Urca process. Hyperons may also constitute a large fraction of the core baryons (see e.g. Glendenning 1985) and will then participate into either modified (Maxwell 1987) or direct (Prakash et al. 1992) Urca processes depending on their relative concentrations, but with somewhat lower emissivities compared to the corresponding nucleon processes. We refer to Pethick (1992) and Prakash (1993) for recent reviews of the neutrino emission problem. While there is still doubt about which fast process can actually occur, the number of presently proposed channels is so large that it is becoming difficult to believe that none of them is permitted and that neutron star cooling follows the old 'standard model' with only the slow modified Urca process. Nevertheless, awaiting for a definite argument on this point we will still consider both the fast and slow cooling scenarios.

Deconfined quarks may be present in the center of massive neutron stars and are also copious neutrino emitters. They thus belong to the fast cooling scenario but obviously require a separate treatment. We will not consider them explicitely here.

3.2 Boundary condition.

An important ingredient is the above mentioned $T_i - T_e$ relationship. Gudmundsson, Pethick & Epstein (1982, 1983) were the first to present a detailed study of it but did not include the effect of the magnetic field $\vec{H}$ which enhances the heat transport parallel to $\vec{H}$ and strongly suppresses it in the perpendicular direction. The

extensive magnetic envelope calculations of Hernquist (1985) and Van Riper (1988) for transport parallel to $\vec{H}$ show that for a given inner temperature T_i the surface temperature T_s is raised, compared to the non magnetic case, but by no more than 50% even with a field of 10^{14} G (The surface magnetic field of Geminga is estimated to be about 1.6×10^{12} G). When the field is at an angle to the surface T_s should be lower, and by simple geometric considerations Hernquist (1985) argued that the magnetic effects when including a global field configuration are probably very small. Schaaf (1990a,b) has performed envelope calculations with an arbitrary orientation of $\vec{H}$ with respect to the surface and his results can be used to estimate the surface temperature distributions $T_s(\theta, \phi)$ resulting from various magnetic field configurations and the corresponding effective temperatures T_e. Preliminary results (Page 1993) confirm Hernquist's point that the $T_i - T_e$ relationship depends only very weakly on the magnetic field. We will consequently use the zero field relationship here which should introduce an error of no more than a few percent.

3.3 High density equation of state.

The equation of state (EOS) has two functions in our models, the first being simply to give the global structure of the star, i.e. the density vs. radius profile as a solution of the Oppenheimer-Volkoff equation of hydrostatic equilibrium, and the second being to determine the chemical composition. Obviously the slow and fast cooling cases are associated with quite different EOS at supranuclear density and we will discuss them separately.

For modeling the slow cooling we consider five different EOS's from modern calculations, relativistic (MPA: Müther, Prakash & Ainsworth 1987), non-relativistic (FP: Friedman & Pandharipande 1981; WFF(av14): Wiringa, Fiks & Fabrocini 1988) and

two parametric EOSs PAL32 & PAL33 (PAL: Prakash, Ainsworth & Lattimer 1988) whose properties are intermediate to the above three. Each one of these calculations gives the energy per baryon for neutron matter and symmetric nuclear matter from which we obtain the EOS for matter in β-equilibrium and the chemical composition following Wiringa et al. (1988), or Prakash, Ainsworth & Lattimer (1988) for PAL. The properties of these EOSs related to neutron stars are summarized in Table 2; they encompass a broad range of stiffness with maximum masses from 1.68 $M_\odot$ to 2.44 $M_\odot$, proton fractions in a 1.4 $M_\odot$ star between 2.0 % and 11.4 % and radii of a 1.4 $M_\odot$ star between 10.6 km to 12.5 km. We have rejected EOSs with proton fractions large enough to allow the direct Urca process in a 1.4$M_\odot$ star, but do consider MPA, PAL32 and PAL33 which allow it at higher masses (notice that the PAL32 EOS gives a 1.4 $M_\odot$ star on the verge of allowing the direct URCA process). Two EOSs, BPS (as listed in Baym, Pethick & Sutherland 1971) and PS (Pandharipande, Pines & Smith 1976) have been very popular in neutron star cooling studies. We do not use the BPS EOS for modelling the slow cooling since this extremely soft EOS (which gives a density above 10 times nuclear matter density in the center of a 1.4 $M_\odot$ star) is actually built on a high density EOS with hyperons (Pandarhipande 1971) in which the hyperonic direct Urca is allowed and this EOS thus belongs to the fast cooling case (hyperons appear at a star mass of 0.4 $M_\odot$ in this model). The softening of this EOS is due to the presence of the hyperons in an essential way and nothing similar can be expected with only nucleons.

The PS EOS has already been considered in previous works (Nomoto & Tsuruta 1986, 1987; VanRiper 1991) and we will simply quote their results below. However, in this extremely stiff EOS the neutrons form a three dimensional lattice, thus having a totally different specific heat and different neutrino emissivity than liquid neutrons,

two facts not taken into account in the models, and the stiffness of this EOS is inseparable from to the lattice structure.

The choice of the EOS for fast cooling models is not as important as for slow cooling at the present stage of development of the theory. There are several other factors which have much more influence, as for exemple the critical density at which fast neutrino emission turns on, which fast neutrino emission is actually at work, the occurence of baryon pairing, etc., all of which are at best poorly known. Therefore calculations of fast cooling have often been done with various EOS in a partially justified careless way. However one model has been developed with much detail, based on the ALS model of dense matter (Takatsuka *et al.* 1978) which is somewhat inspired from the PS EOS, but where the lattice structure is one-dimensional and where two-dimensional nucleon pairing occurs in planes orthogonal to the lattice direction (see Tamagaki 1992 for a general description). In this model charged pion condensation develops at high density but the resulting EOS is close to the FP EOS at low density below the condensation threshold, i.e. the stiffness of the PS EOS has disappeared. Cooling calculations within the ALS model have been performed by Umeda *et al.* (1993b) (as shown in Tamagaki 1992) and their results will be used below.

3.4 Nucleon pairing.

Pairing *à la* BCS (superfluidity) of the nucleons in the neutron star core has a dramatic effect on the cooling, because it suppresses both the neutrino emission and the specific heat. The pairing is in the $^1S_0$ partial wave at low density and then shifts to the $^3P_2$ partial wave at higher density. The protons in the core and the neutrons in the inner crust are expected to be paired in the $^1S_0$ partial wave while the neutron

pairing shifts to the $^3P_2$ partial wave in the core. Pairing of protons in the $^3P_2$ partial wave seems to have never been considered, probably on the ground that its critical temperature would be very low. At still higher densities the pairing should shift to $^1D_2$ partial wave (the next partial wave in which the free nucleon-nucleon interaction is attractive) but the corresponding critical temperature as been estimated to be too low to make this type of pairing of any interest (Amundsen & Østgaard 1985b). Theoretical calculations of T_c are extremely difficult and the presently published values are still highly uncertain except in the case of crust neutrons $^1S_0$ pairing where reasonable agreement has been obtained between the various latest calculations. Figure 1 shows most of the presently published calculations of critical temperatures for core neutron and proton pairing. One sees from it that both the maximum value of T_c and the density range where it is non zero are very uncertain, particularly in the neutron case. For the $^1S_0$ proton pairing the latest calculation (Wambach, Ainsworth & Pines 1991) was the first one to include in a consistent way the neutron background and shows a strong *reduction* of T_c, but with an apparently different density dependence compared to the earlier calculations. However this result depends strongly on the relative densities of neutrons and protons and thus calculations with a different proton fraction (a poorly known quantity) may give quite different results (Ainsworth 1992). Medium dispersion effect, i.e. change in the nucleon effective mass, have an enormous effect as shown in Figure 1b by the difference between the curves AO and T72 where the effective mass $m^* \equiv M^*/M$ is obtained in a self consistent way and the corresponding curves labelled with $m^* = 1$ for which the effective mass is forced to the free mass value. (The Hoffberg *et al.* 1970 calculation used $m^* = 1$). Of course m^* is also poorly known at high density. Further extensive calculations within the ALS model (Takatsuka & Tamagaki 1982 and references therein) with and without pion

condensation give values of T_c for $^3P_2$ neutron pairing in between the two extremes shown in Figure 1b as T72 and T72($m^* = 1$). For $^3P_2$ neutron pairing, background effects beyond the first order ones considered in the results shown in Fig. 1b and similar to the effects considered by Wambach, Ainsworth & Pines (1991) for $^1S_0$ proton pairing have been studied (Jackson *et al.* 1982). The results indicate that in this case background effects strongly *enhance* the pairing; thus values of T_c higher than shown in the figure and extending to higher densities are quite possible. In this light the case for proton $^3P_2$ pairing should also be considered seriously as well as $^1D_2$ pairing. In other words we know neither the value of T_c in the core nor the relevent density range, for both neutron and protons, but large values extending up to high densities can be reasonably expected.

If hyperons are presents one can expect that they will also pair for the same reasons as nucleons do. With regard to quarks, pairing is also very probable (Bailin & Love 1984).

The effect of pairing is to reduce the phase space available for excitations. As a result both the specific heat of the paired component and the neutrino processes to which it participates will be suppressed. We treat this effect on C_v following Levenfish & Yakovlev (1992) (see also Gnedin & Yakovlev 1993) who performed detailed calculations of the reduction factors in both cases of isotropic $^1S_0$ and anisotropic $^3P_2$ pairing. For the neutrino emission suppression we simply use a Boltzmann factor $\exp(-\Delta/kT)$, where Δ is the pairing gap, which is not very accurate but has no serious consequence here since we are considering the photon cooling era only.

4. FAST NEUTRINO COOLING SCENARIOS

Fast neutrino cooling encompasses a variety of different scenarios, kaon or pion condensate, direct Urcas with nucleons and/or hyperons and/or isobars, quark matter, etc, which share the common characteristics that their neutrino emissivities are many orders of magnitude higher than the modified Urca process emissivity. As a result, whenever one of these processes is allowed to operate freely the resulting surface temperature, once the star has reached isothermality, is much below any of the presently available observational estimates (Page & Baron 1990; VanRiper 1991; Page & Applegate 1992; Page 1992; Umeda *et al.* 1993b), including the new Geminga case. This raw picture is strongly altered if the neutrino emitting baryons (nucleons, hyperons, quarks, etc.) become paired. As presented by Page (1989) for the kaon condensate case and Page & Applegate (1992) for the nucleon direct Urca the early suppression of the neutrino emission due to the pairing gap can keep the surface temperature T_s, after isothermalization and until an age of about 10^5 years, anywhere between approximately 2×10^5 K and 1.5×10^6 K. The actual value of T_s is then only a function of the pairing critical temperature T_c of the neutrino emitting fluid(s) (to be precise, since T_c is density dependent, T_s is a function of the lowest value of T_c within the 'pit' of fast neutrino emission). In a multicomponent system like nucleons + hyperons, various direct Urca processes can operate simultaneously (Prakash et al. 1992) and all of them have to be stopped by having one of the participating baryons paired for the star not to drop into invisibility. In particular, if both Λ and Σ^- are present together they undergo a purely hyperonic direct Urca process and thus one of them must be paired. One can expect that T_c is lower for hyperons than for nucleons if the former have weaker interactions than the latter, and the star's temperature

would then be controlled by hyperon pairing.

The models of Page & Baron (1990), Umeda *et al.* (1993b) and Page & Applegate (1992) of kaon, pion and nucleon direct Urca cooling respectively with superfluidity suppression easily accomodate the estimated surface temperature of Geminga. The crucial point however is that pairing has to occur down to the very center of the star and the critical temperature must be higher than 10^9 K everywhere. If even a very small region is left unpaired it will drive the surface temperature well below the observed value of 5×10^5 K. For example, the 1.4 $M_\odot$ case of Page & Applegate (1992) with a direct Urca emitting pit of only 0.038 $M_\odot$ has a temperature of 1.5×10^5 K at Geminga's age if pairing does not occur. Such a low surface temperature would make Geminga's surface practically unobservable by ROSAT (the hot polar cap would of course still be seen).

It is not possible to distinguish between the various neutrino emission processes from this analysis only: both a kaon (or pion) condensates or the direct Urca, even if their emissivities differ by three orders of magnitude, are compatible with the Geminga data when pairing is taken into account, but with different values for T_c. The T_c values needed are within the range of the theoretical predictions, but this range is so large that it can accomodate almost any data. Moreover, even within one given neutrino emission scheme very different values of T_c are possible : e.g. the model labelled HGRR and 0.1HGRR of Fig. 2 in Page & Applegate (1992), i.e. direct URCA and $^3P_2$ neutron pairing with T_c from Hoffberg *et al* (1970) or the same T_c multiplied by 0.1, are both acceptable within the observational uncertainty in the Geminga data.

It should be mentioned that internal heating by friction of the crust neutron superfluid can significantly alter the thermal evolution of a neutron star when its

temperature, thus its specific heat, is low. The models of fast coling with pions and reheating of Umeda *et al.* (1993a), without core nucleon pairing, can produce a star with a surface temperature, at Geminga's age, of at most 3×10^5 K *when reheating is at its maximum strengh* (instead of 1.5×10^5 K without reheating). This is lower that the Geminga temperature considered here (measured with a black-body spectrum) but may be high enough if Geminga is actually cooler.

5. SLOW NEUTRINO COOLING SCENARIO

The slow neutrino cooling scenario is a well defined scenario based on the conservative hypothesis that the neutron star core is made exclusivelly of neutrons and protons (plus electrons and muons to preserve charge neutrality, but no charged pions, kaons, quarks, etc...) with a proton fraction low enough for the direct Urca process to be forbidden (Lattimer *et al.* 1991), and its predictions for surface temperatures are much more restrictive than in the fast neutrino cooling case. We defer a detailed study to later work and only analyze here the photon cooling era relevant to Geminga.

The photon energy loss can be calculated accurately since the core temperature-surface temperature relationship is known quite accurately, even in presence of magnetic field. We take the core neutrino emissivity of the modified Urca process and the two associated neutral current bremstrahlung processes from Friman & Maxwell (1979). Of critical importance here is the total specific heat of the star, which depends on the EOS and chemical composition (proton fraction). Pairing of nucleons is essential here because of its suppression of the specific heat. Table 3 shows the contribution to the normal (i.e. without pairing) specific heat of the various components

in a 1.4 $M_\odot$ star at a temperature $T = 10^9 K$ for our five EOSs. Pairing will suppress C_v exponentially when $T \ll T_C$ and the corresponding specific heat will practically disappear. In all our calculations the crust neutrons are paired using the gap from Ainsworth, Wambach & Pines (1989) and their contribution to C_v is thus strongly reduced; the crust electrons have a negligible contribution as well as the crust lattice. One can see from the table that the core neutrons contribute about $\frac{3}{4}$ of the total specific heat, the protons $\frac{1}{4}$ and the core electrons about 5 %, independently of the EOS.

Due to the large theoretical uncertainty on the actual value of the pairing critical temperature T_c for both neutrons and protons in the core as well as the uncertainty on the density dependence of T_c we first consider density independent T_c, i.e. we force pairing in the whole core and take $T_c = 2 \times 10^9$ K. The resulting cooling curves of a 1.4 $M_\odot$ for our five EOSs are shown in Figure 2a-2d and compared with the Geminga data. Because in this photon cooling era the determining factor is the total specific heat, the five EOSs give basically identical results since the contribution of the various components to C_v is only weakly dependent on the EOS and pairing, when assumed, is present in the whole core. When none of the core nucleons is paired (a) the theoretical results are consistent only with the higher surface temperature T_s and the older age: taking into account that this T_s is certainly an overestimate one can state that Geminga's temperature is incompatible with these cooling models (unless Geminga's age is underestimated). With pairing of the protons (b) the discrepancy increases because the small ($\sim$ 25%) decrease of the specific heat in the photon cooling era is not sufficient to compensate the significant reduction of the earlier core neutrino emission (during which only the very slow *nn* bremstrahlung is unaffected) which gives a high temperature at the beginning of the photon cooling era. When all

the core neutrons are paired (c) the reduction of C_ν is large enough to accomodate the observed temperature. If both neutrons and protons are paired within the whole core (d) C_ν is cut by a factor 20 (only the electron contribution is left) and the temperature drop during the photon cooling era is extremely fast; however reheating mechanisms (Shibazaki & Lamb 1989; Cheng et al. 1992; Umeda *et al.* 1993a) could slow the cooling and keep the temperature compatible with Geminga. These results were at a fixed mass of 1.4 $M_\odot$, but Figure 3 shows that changing the star mass makes little difference as long as the pairing is still assumed throughout the whole core.

Figure 4 shows three cooling curves with three published calculations of $^3P_2$ neutron pairing and the EOS WFF(av14) for a 1.4 $M_\odot$ star. (The Fermi momentum of the neutrons in the center of the star, for comparison with Figure 1, is $k_F(n) = 2.58 fm^{-1}$). The pairing of Takatsuka (1972) has almost no effect since T_c vanishes at low density and most of the core in left unpaired. The two calcualtions of Hoffberg *et al.* (1970) and Amundsen & Ostgaard (1985b) give almost identical results in the photon cooling era since in both cases the whole core is paired and the internal temperature T_i is much lower than T_c; in both cases the whole core neutron specific heat has been practically eliminated. In the neutrino cooling era where T_i is higher these two cases do differ significantly (their T_c differ by an order of magnitude): in the Hoffberg *et al.* (1970) case the core neutrino emission is practically turned off early on due to the very high T_c, while in the Amundsen & Ostgaard (1985b) case the suppression has happened much later and is less efficient. It is hence not possible to deduce any value for T_c from the Geminga data only, besides that it must be higher than a few times 10^8 K, but we can state that pairing must occur within most of the core.

Published cooling curves with the PS EOS (Nomoto & Tsuruta 1986, 1987; Van-Riper 1991) also fit the Geminga data in their superfluid versions, as well as the

standard cooling curve of Umeda *et al.* (1993b) which also have neutron pairing in the whole core.

6. COMMENTS

The surface temperatures we have obtained with the slow neutrino cooling scenario during the photon cooling era when both neutrons and protons are paired within the whole core (Figure 2d) are much lower than any prediction previously published. It simply comes from the fact that 95 % of the star specific heat has been suppressed by superfluidity when all core nucleons are paired. This case has to be seriously considered for low mass neutron stars, where there is little doubt that pairing happens down to the center of the star for both neutrons and protons, and it has some unexpected effects. Consider for example, as shown in Figure 5, the case of a heavy star undergoing fast neutrino cooling with suppression from neutron $^3P_2$ pairing but whose core has still a substantial amount of unpaired protons. If the critical temperature for neutron pairing is a few times 10^9 K the star will have a lower temperature during the neutrino cooling era than a slow neutrino cooling star of low mass but later during the photon cooling era it will be much warmer than the lighter (wholly paired) star. Thus *fast neutrino cooling does not mean fast cooling forever.*

If one adopts the idea that the critical density for the onset of fast neutrino emission is low then it is quite possible that all neutron stars undergoing slow neutrino cooling, thus having very low central densities, have both their neutrons and protons paired within the whole core with high values of T_c. All neutron stars undergoing slow neutrino cooling would then cool very fast in the photon cooling era and become

invisible after a couple of hundred of thousands of years. Consequently, any neutron star older than that with detectable surface thermal emission has an unpaired baryonic core component, which provides the star with a sizable specific heat, but has undergone fast neutrino emission suppressed early on by pairing of its other(s) core component(s).

However, there may not even be such a thing as a slow neutrino cooling ('standard cooling') neutron star since, as mentioned in the introduction, the number of presently proposed channels for fast neutrino emission is so large, and the corresponding critical densities so low in some cases, that it is possible that *all* neutron stars cool by some fast neutrino process. If this is the case the thermal evolution of all neutron stars is entirely controlled by superfluidity. The surface temperature from age $\sim 10^2$ years to $\sim 10^5$ years depends on the minimal value of T_c for the relevent neutrino emitting baryonic component (nucleon or hyperon) in the core (Page & Applegate 1992) and the temperature for ages between $\sim 10^5$ years till $\sim 10^6$ years depends on how much of the core is left unpaired. It is worth mentioning here that the observational support for the 'standard model' is actually extremely dim, if not nonexistent. It has traditionally been based (Tsuruta 1986) on *EINSTEIN* observations of the Crab pulsar (Harden & Seward 1984) and of the two compact objects detected in the supernova remnants 3C58 (Becker, Helfand & Szymkowiak 1982) and RCW103 (Tuohy *et al* 1983), all three having ages around 1000 years and upper limits on the temperature of the order of $2 - 3 \times 10^6$ K. However none of these three temperatures estimates can be given much credibility for the following reasons : 1) ROSAT has failed to detect the previously seen source in RCW103 (Becker *et al* 1993); no matter what this object is, or was, it is not a neutron star cooling according to the slow neutrino emission scenario. 2) The temperature estimate of the 3C58 central source was based on an

assumed distance of 8 kpc which was later reduced by a factor 3 (Green & Gull 1982): with this new distance the resulting temperature would be low enough to be marginally inconsistent with the 'standard' cooling model. Moreover the age of 3C58 is based on an association with the A.D. 1191 supernova, but Becker, Helfand & Szymkowiak (1982) questioned this association arguing from the low ratio of X-ray to radio luminosities of the remnant that it is probably much older; this would ruins its relevance for comparison with models of early cooling of neutron stars. 3) As for the Crab pulsar (the only case of these three whose existence and age are beyond doubt) the temperature is based on an upper limit of the flux between the pulses of the X-ray curve observed by *EINSTEIN* : the pulsar is *undetected* at this phase and the temperature can hence be anywhere below the reported upper limit of 2.5×10^6 K. In none of these three cases was there any spectral evidence that the X-ray emission is thermal emission from the surface of the star since the Crab and RCW103 observations were done with the HRI detector which had no energy resolution and the count rate from the 3C58 point source in the IPC detector was too low to provide usefull spectral information. Moreover the magnetospheric X-ray emission from such young neutron stars is so strong that there is little hope for detection of thermal radiation from the surface of the star itself (Õgelman 1993). A fourth neutron star young enough to allow us to distinguish between slow and fast neutrino cooling, and in this case with good data, is PSR 0833-45 (Vela): comparisons with theoretical models have shown repeatedly that its surface temperature is too low for the 'standard' cooling and requires a fast cooling agent (Nomoto & Tsuruta 1986, Shibazaki & Lamb 1989, Page & Baron 1990, Van Riper 1991, Page & Applegate 1992, Umeda *et al* 1993a). It is hence a reasonable theoretical *a priori* to interpret all data within the fast neutrino cooling scenario. Nevertheless, as stated in section 3.1,

we still consider both types of neutrino cooling, letting observation be the ultimate judge.

Since analyses of the ROSAT observations of PSR 0656+14 and PSR 1055-52 have been published recently we will now briefly comment on these results in light of the preceding remarks. In the case of PSR 0656+14, when the spectral fit is done with a black-body the resulting surface temperature is $9.0 \pm 0.4 \times 10^5$ K while a pure He atmosphere gives $2.2 \pm 0.2 \times 10^5$ K (Finley, Ögelman & Kiziloğlu 1992). For a spin-down age of 1.1×10^5 years the first value is perfectly compatible with the slow neutrino cooling scenario (with or without core pairing) while the second one is in complete disagreement and needs fast neutrino cooling. An analysis with a magnetic hydrogen atmosphere spectrum gives an intermediate value of $6.9^{+0.5}_{-0.3} \times 10^5$ K (Anderson *et al.* 1993) which is lower than what previously predicted for slow neutrino cooling but is still just compatible with our new results in the case of complete pairing of the core (Figure 2d). However if PSR 0656+14 is younger than its spin-down age indicates then the magnetic temperature estimate is below all our models of slow neutrino cooling and a fast cooling agent is necessary. A younger age is not impossible since PSR 0656+14 has been identified as the result of the supernova which produced the Monogem Ring (Nousek *et al.* 1981; Thompson *et al.* 1991), and comparison with supernova remnant models gives it an age of $6 - 9 \times 10^4$ years. For PSR 1055-52, spectral fits with a black-body give a surface temperature of $(7.0 \pm 0.6) \times 10^5$ K (Ögelman & Finley 1993). Given the spin-down age of 5×10^5 years, Ögelman & Finley conclude that this temperature is compatible with the slow neutrino cooling models, but only for models *without pairing in the core.* This temperature is too high compared to the slow cooling when neutron core pairing is included, but reheating may explain the discrepancy and moreover fits with non black-body spectra will give

lower temperatures and require less reheating. If both neutrons and protons are paired within the whole core the theoretical temperature with slow neutrino cooling is much lower than the 7×10^5 K reported. When comparing with the reheating models of Shibazaki & Lamb (1989) or Cheng *et al* (1992) and Chong & Cheng (1993) only their maximum reheating rates could justify the discrepancy in this case: PSR 1055-52 most probably contains an unpaired component in its core. If one adopts the idea that the critical density for fast neutrino emission is low and that all neutron stars undergoing slow neutrino cooling have their whole core paired and thus follow the trajectory of Fig. 2d) then this reported temperature of 7×10^5 K is incompatible with the slow neutrino cooling scenario unless a very efficient reheating mechanims is at work.

7. CONCLUSIONS

We have compared the recent temperature measurement of the Geminga neutron star with cooling models and found that, since this star is old enough to be in the photon cooling era, both fast and slow neutrino emission mechanisms can explain it. One therefore cannot draw any conclusion about neutrino emission from dense nuclear matter using this observation only. However, *a crucial feature in both types of models is that they need nucleon pairing in most, if not all, of the core.* If no pairing is assumed in the core then the predicted temperature is either too high (slow neutrino cooling) or too low (fast neutrino cooling) compared to the observed temperature of Geminga.

With fast neutrino cooling nucleon pairing is needed to stop the early cooling which, without this, would produce a star of temperature much lower than what

is observed. If the fast neutrino emission is from hyperonic processes it is possible that the suppression we observe is due to hyperon superfluidity. It is not possible to distinguish between the various fast processes however, the theoretical uncertainty on T_c allowing us to accomodate very different neutrino emission rate. Moreover, within one given fast cooling scenario the observational uncertainty also allows very different values of T_c. However, since fast neutrino emission occurs down to the very center of the core these scenarios need, to be compatible with the Geminga observation, pairing up to the highest density reached in this object, with pairing critical temperatures higher than 10^9 K.

Within the slow neutrino cooling model ('standard model') superfluidity is also needed, but for a different reason. The observed temperature is below what the simple model without pairing predicts, but since this star is cooling by photon emission we can accelerate the cooling at this time by decreasing the specific heat through pairing. The theoretical curves, in the photon cooling era, are very insensitive to the high density EOS or the star mass, the only determining factor being how much of the core specific heat has been eliminated by pairing. If we accept an age of 3×10^5 years and a temperature of 5×10^5 K then the specific heat must have been reduced to about 25% of its normal value. This can be obtained either by pairing of the neutrons in the whole core or by a combination of both neutron and proton pairing, but even in this case most of the neutrons must be paired. If both neutrons and protons are paired in the whole core photon cooling becomes so efficient that a substantial amount of reheating is needed, but several possible mechanisms have been proposed and may be able to provide sufficient reheating.

The above discussion shows that in order to distinguish clearly between the fast and slow neutrino cooling scenarios we need observations of neutron stars younger

than 5×10^4 years where the slow cooling scenario predicts temperatures higher than 0.9 to 1.1 $\times 10^6$ K, depending on the exact age, while at later times both scenarios can accomodate most observable temperatures depending on the amount of pairing assumed. Geminga is old enough that the effect or the early neutrino cooling has been washed out, however our analysis showed that this star does tell us, independently of its earlier neutrino cooling history that most, if not all, of its core is paired. PSR 0656+14 is at the limit where we could still distinguish the effect of fast neutino cooling but the present uncertainty on its temperature precludes drawing any conclusion. PSR 1055-52 can be also interpreted within both types of neutrino scenarios but its core must contain an unpaired component whose specific heat keeps the star warm despite of its age. If one accepts the fast neutrino cooling scenario as universal (a reasonable theoretical *a priori*) then these three objects show evidence of baryon pairing down to their very center, needed for suppression of the early neutrino emission, but none of them requires this scenario.

ACKNOWLEDGEMENTS

I am gratefull to T. Ainsworth, J. H. Applegate, J. P. Halpern, M. Prakash and M. Ruderman for discussions. This work was supported by a HEA-NASA grant NAGW 3075 and in its early phase by a fellowship from the Swiss National Science Fundation.

Process Name	Process	Emissivity Q_ν (erg/sec/cm^3)
a) Modified URCA	$\begin{cases} n + n' \rightarrow n' + p + e^- + \overline{\nu_e} \\ n' + p + e^- \rightarrow n' + n + \nu_e \end{cases}$	$\sim 10^{20} \cdot T_9^8$
b) K-condensate	$\begin{cases} n + K^- \rightarrow n + e^- + \overline{\nu_e} \\ n + e^- \rightarrow n + K^- + \nu_e \end{cases}$	$\sim 10^{24} \cdot T_9^6$
c) π - condensate	$\begin{cases} n + \pi^- \rightarrow n + e^- + \overline{\nu_e} \\ n + e^- \rightarrow n + \pi^- + \nu_e \end{cases}$	$\sim 10^{26} \cdot T_9^6$
d) Direct URCA	$\begin{cases} n \rightarrow p + e^- + \overline{\nu_e} \\ p + e^- \rightarrow n + \nu_e \end{cases}$	$\sim 10^{27} \cdot T_9^6$
e) Quark URCA	$\begin{cases} d \rightarrow u + e^- + \overline{\nu_e} \\ u + e^- \rightarrow d + \nu_e \end{cases}$	$\sim 10^{26} \alpha_c T_9^6$

Table 1: **Some core neutrino emission processes and their emissivities.**

The emissivities are from : a) Friman & Maxwell 1979, b) Brown *et al* 1988, c) Maxwell *et al* 1977, d) Lattimer *et al* 1991 and e) Iwamoto 1980. T_9 is the temperature in units of 10^9 kelvins.

EOS	Maximum mass star			1.4 $M_\odot$ star		
.	$M_{max}(M_\odot)$	$\rho_{max}(fm^{-3})$	$x_p(\%)$	$R(km)$	$\rho_c(fm^{-3})$	$x_p(\%)$
FP	1.79	1.18	~ 0	10.85	0.69	2.0
WFF(av14)	2.10	1.25	4.8	10.60	0.64	9.6
MPA	2.44	0.89	19.0	12.45	0.41	9.0
PAL32	1.68	1.51	15.2	11.02	0.74	11.4
PAL33	1.90	1.24	14.0	11.91	0.54	9.7

Table 2: **Some properties of the EOS's used for slow neutrino cooling.**

Columns two to four list the mass, central density and central proton fraction of a maximum mass star. Columns five to seven give properties of a 1.4$M_\odot$ star : radius, central density and central proton fraction. (The PAL EOS's are labelled PALij, i,j=1,2,3, where i refers to the symmetry energy function and j to the compression modulus)

EOS	Core components			Crust components	
.	n	p	e	n	e
FP	9.89	2.89	0.50	0.97	0.025
WFF(av14)	9.31	2.81	0.51	0.72	0.018
MPA	11.90	3.90	0.67	1.60	0.044
PAL32	9.66	3.41	0.68	1.16	0.031
PAL33	10.96	3.72	0.68	1.42	0.037

Table 3: **Contributions to the specific heat.**

Normal specific heat. at $T = 10^9$ K, of neutrons, protons and electrons in the core nd crust of a 1.4 $M_\odot$ neutron star built with the five EOS's used for slow neutrino ooling. (Units are 10^{38} $ergs\ K^{-1}$, i.e. $C_v(T) = (\text{Table} - \text{Entry}) \times (T/10^9 K) \times 0^{38}\ ergs\ K^{-1}$).

REFERENCES

Ainsworth, T. L. 1992, private communication

Ainsworth, T. L., Wambach, J. & Pines, D. 1989, Phys. Lett., B222, 173

Amundsen, L. & Østgaard, E. 1985a, Nucl. Phys., A437, 487

Amundsen, L. & Østgaard, E. 1985b, Nucl. Phys., A442, 163

Anderson, S. B., Córdova, F. A., Pavlov, G. G., Robinson, C. R. & Thompson, Jr, R. J. 1993, ApJ, submitted

Bailin, D. & Love, A. 1984, Phys. Rep., 107, 325

Baym, G., Pethick, C. J. & Sutherland, P. 1971, ApJ, 170,299

Becker, R. H., Helfand, D. J. & Szymkowiak, A. E. 1982, ApJ, 255, 557

Becker, W., Trümper, J., Hasinger, G. & Aschenbach B. 1993, in Isolated Pulsars, ed. K. A. Van Riper, R. Epstein & C. Ho (Cambridge : Cambridge University Press)

Bignami, G. F. & Caraveo, P. A. 1992, Nature, 357, 287

Brown, G. E., Kubodera, K., Page, D. & Pizzochero, P. 1988, Phys. Rev., D37, 2042

Chao, N.-C., Clark, J. W. & Yang, C.-H. 1972, Nucl. Phys., A179, 320

Cheng, K. S., Chau, W. Y., Zhang, J. L. & Chau, H. F. 1992, ApJ, 396, 135

Chong, N. & Cheng, K. S. 1993, preprint

Finley, J. P., Õgelman, H. & Kiziloğlu, Ü 1992, ApJ, 394, L21

Friedman, B. & Pandharipande, V. R. 1981, Nucl. Phys., A361, 502

Friman, B. L. & Maxwell, O. V. 1979, ApJ, 232, 541

Glendenning, N. K. 1985, ApJ, 293, 470

Gehrels, N. & Chen, W. 1993, Nature, 361, 706

Gnedin, O. Y. & Yakovlev, D. G. 1993, Pisma v Astron. Zh. (Sov. Astron. Lett.), 19, (March 1993 issue)

Green, D. A. & Gull, S. F. 1982, Nature, 299, 606

Gudmundsson, E. H., Pethick, C. J. & Epstein, R. I. 1982, ApJ, 259, L19

Gudmundsson, E. H., Pethick, C. J. & Epstein, R. I. 1983, ApJ, 272, 286

Halpern, J. P. and Holt, S. S. 1992, Nature, 357, 222

Halpern, J. P. & Ruderman, M. 1993, ApJ, submitted

Harnden, F. R. & Seward, F. D. 1984, ApJ, 283, 279

Hernquist, L. 1985, MNRAS, 213, 313

Hoffberg, M., Glassgold, A. E., Richardson, R. W. & Ruderman, M. 1970, Phys. Rev. Lett., 24, 775

Iwamoto, N. 1980, Phys. Rev. Lett.,44, 1637

Jackson, A. D., Krotscheck, E., Meltzer, D. E. & Smith, R. A. 1982, Nucl. Phys., A386, 125

Lattimer, J. M., Pethick, C. J., Prakash, M. & Haensel, P. 1991, Phys. Rev. Lett., 66, 2701

Levenfish, K. P. & Yakovlev, D. G. 1993a, in Strongly Coupled Plasma Physics, ed. H. M. Van Horn & S. Ichimaru (Rochester: University of Rochester Press)

Lyne, A. G. & Graham-Smith, F. 1990, Pulsar Astronomy, (Cambridge: Cambridge University Press)

Maxwell, O. V. 1987, ApJ, 316, 691

Maxwell, O. V., Brown, G. E., Campbell, D. K., Dashen, R. F. & Manassah, J. T. 1977, ApJ, 216, 77

Michel, F. C. 1991, Theory of Neutron Star Magnetospheres, (Chicago: The University of Chicago Press)

Miller, M. C. 1992, MNRAS, 255, 129

Müther, H., Prakash, M. & Ainsworth, T. L. 1987, Phys. Lett., B199, 469

Niskanen, J. A. & Sauls, J. A. 1981, Preprint

Nomoto, K. & Tsuruta, S. 1986, ApJ, 305, L19

Nomoto, K. & Tsuruta, S. 1987, ApJ, 312, 711

Nousek, J. A., Cowie, L. L., Hu, E., Lindblad, C. J. & Garmire, G. P. 1981 ApJ, 248, 152

Ögelman, H., 1991, in Neutron Stars: Theory and Observation, ed. J. Ventura & D. Pines (Dordrecht: Kluwer Academic Publisher)

Ögelman, H., 1993, in Isolated Pulsars, ed. K. A. Van Riper, R. Epstein & C. Ho (Cambridge : Cambridge University Press)

Ögelman H. & Finley J. P. 1993, ApJ, 413, L31

Ögelman, H., Finley, J. P. & Zimmerman, H. U. 1993, Nature, 361, 136

Page, D. 1989, Ph.D. Thesis, Stony Brook

Page, D. 1992, in Proceeding of the First Symposium on Nuclear Physics in the Universe, ed. M. R. Strayer & M. W. Guidry (Bristol: Adam Hilger & Co.)

Page, D. 1993, In preparation

Page, D. & Applegate, J. H. 1992, ApJ, 394, L17

Page, D. & Baron, E. 1990, ApJ, 354, L17; Erratum in ApJ, 382, L111

Pandharipande, V. R. 1971, Nucl. Phys., A178, 123

Pandharipande, V. R., Pines, D. & Smith, R. A. 1976, ApJ, 208, 550

Pethick, C. J. 1992, Rev. Mod. Phys., 64, 1133

Prakash, M. 1993, in Proceeding of International Conference on 'Realistic Nuclear Structure', to be published in Phys. Rep.

Prakash, M., Ainsworth, T. L. & Lattimer, J. M. 1988, Phys. Rev. Lett., 61, 2518

Prakash, M., Prakash, M., Lattimer, J. & Pethick, C. J. 1992, ApJ., 390, L77

Romani, R. W. 1987, ApJ, 313, 718

Schaaf, M. E. 1990a, A&A, 227, 61

Schaaf, M. E. 1990b, A&A, 235, 499

Shibanov, Y. A., Zavlin, V. E., Pavlov, G. G. & Ventura, J. 1992, A&A, 266, 313

Shibazaki, N. & Lamb, F. K. 1989, ApJ, 346, 808

Takatsuka, T. 1972, Prog. Theor. Phys., 48, 1517

Takatsuka, T. 1973, Prog. Theor. Phys., 50, 1754

Takatsuka, T. & Tamagaki, R. 1982, Prog. Theor. Phys., 67, 1649

Takatsuka, T., Tamiya, K., Tatsumi, T. & Tamagaki, R. 1978, Prog. Theor. Phys., 59, 1933

Tamagaki, R. 1992, Physica, B178, 13

Thompson, R. J., Córdova, F. A., Hjellming, R. M. & Fomalont, E. B. 1991, ApJ, 366, L83

Tsuruta, S. 1986, Comments Astrophys, 11,151

Tuohy, I. R., Garmire, G. P., Manchester, R. N. & Dopita, M. A. 1983, ApJ, 268, 778

Umeda, H., Nomoto, K., Tsuruta, S., Muto, T. & Tatsumi, T. 1993b, in preparation, as shown in Tamagaki 1992

Umeda, H., Shibazaki, N., Nomoto, K. & Tsuruta, S. 1993a, ApJ, 408, 186

VanRiper, K.A. 1988, ApJ, 329, 339

VanRiper, K. A. 1991, ApJSuppl, 75, 449

Wambach, J., Ainsworth, T. L. & Pines, D. 1991, in Neutron Stars : Theory and Observation, ed. J. Ventura & D. Pines (Dordrecht: Kluwer Academic Publisher)

Wiringa, R. B., Fiks, V. & Fabrocini, A. 1988, Phys. Rev., C38, 1010

Figures captions

Figure 1. a) Proton $^1S_0$ pairing critical temperatures. CCY : Chao, Clark & Yang 1972, T : Takatsuka 1973, NS : Niskanen & Sauls 1981, AO : Amundsen & Østgaard 1985a, WAP : Wambach, Ainsworth & Pines 1991.
b) Neutron $^3P_2$ pairing critical temperatures. HGRR : Hoffgerg *et al* 1970, T : Takatsuka 1972, AO : Amundsen & Østgaard 1985b. The two dashed curves show the results of T & AO when the neutron effective mass is fixed at the free mass value. In abscissa is the Fermi wave number k_F, related to the particle number density n_i by $k_F(n_i) = (3\pi^2 n)^{1/3} = 1.68(n_i/n_0)^{1/3}\mathrm{fm}^{-1}$ where $n_0 = 0.16\mathrm{fm}^{-3}$.

Figure 2. Cooling by the modified Urca process : effect of the specific heat suppression by nucleon pairing. The various curves correspond to the five EOSs we use : FP continuous, WFF(av14) dashed, MPA dotted, PAL32 dashed-dotted and PAL33 dashed-triple dotted lines. 1.4 $M_\odot$ star.
a) No core pairing at all.
b) Protons paired with a density independent $T_c = 2 \times 10^9$ K.
c) Core neutrons paired with a density independent $T_c = 2 \times 10^9$ K.
d) Protons and core neutrons paired with a density independent $T_c = 2 \times 10^9$ K. Crust neutrons paired according to Ainsworth, Wambach & Pines 1989. The temperature in ordinate is the effective temperature 'at infinity' i.e. red-shifted. The cross shows the Geminga temperature and age.

Figure 3. Cooling by the modified Urca process : effect of the star mass. EOS WFF(av14) and star mass of 1.2 $M_\odot$ (dash-dot), 1.4 $M_\odot$ (continuous), 1.6 $M_\odot$ (dash-double dot) and 1.8 $M_\odot$ (dash) with the same pairings as in Figure 2. Crust neutrons

paired according to Ainsworth, Wambach & Pines 1989. The temperature in ordinate is the effective temperature 'at infinity' i.e. red-shifted. The cross shows the Geminga temperature and age.

Figure 4. Cooling by the modified Urca process : density dependent T_c. EOS WFF(av14) and star mass 1.4 $M_\odot$. The continuous curve has no core neutron pairing, the other three curves have core neutron pairing as labelled (see Figure 1b for the labels). Core protons are not paired. Crust neutrons paired according to Ainsworth, Wambach & Pines 1989. The temperature in ordinate is the effective temperature 'at infinity' i.e. red-shifted. The cross shows the Geminga temperature and age.

Figure 5. Fast neutrino cooling is not fast cooling forever : the curves show the cooling history of two neutron stars of very different masses built with the same EOS, WFF(av14), and the same pairings (HGRR for core neutrons, CCY-PSi) for core protons, as labelled in Figure 1, and Ainsworth, Wambach & Pines 1989 for crust neutrons). With this choice of pairings, neutrons are paired in the whole core for both stars as well as protons in the lighter star while the heavier star has a central region of unpaired protons. We have assumed that a kaon condensate develops above a density of $10^{15} gm/cm^3$ such that the 1.6 $M_\odot$ star has a kaon 'pit' of 0.56 $M_\odot$ while the 1.0 $M_\odot$ star undergoes 'standard' cooling. During the neutrino cooling era ($30yrs < age < 3 \times 10^4 yrs$) the lighter star is warmer due to its low neutrino emission while during the photon cooling era the heavier star is warmer due to its larger specific heat provided by its unpaired protons.

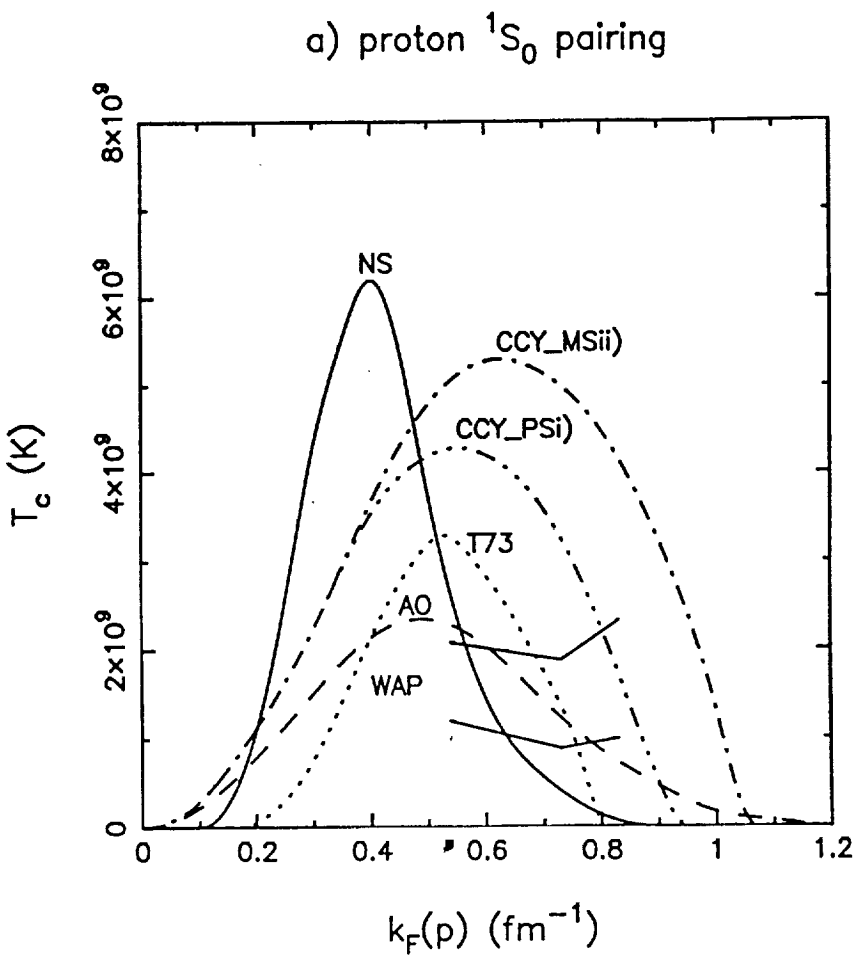
a) proton $^1S_0$ pairing
T_c (K)
$k_F(p)$ (fm^{-1})
NS
CCY_MSii)
CCY_PSi)
T73
AO
WAP
0
2x10^9
4x10^9
6x10^9
8x10^9
0.2
0.4
0.6
0.8
1
1.2

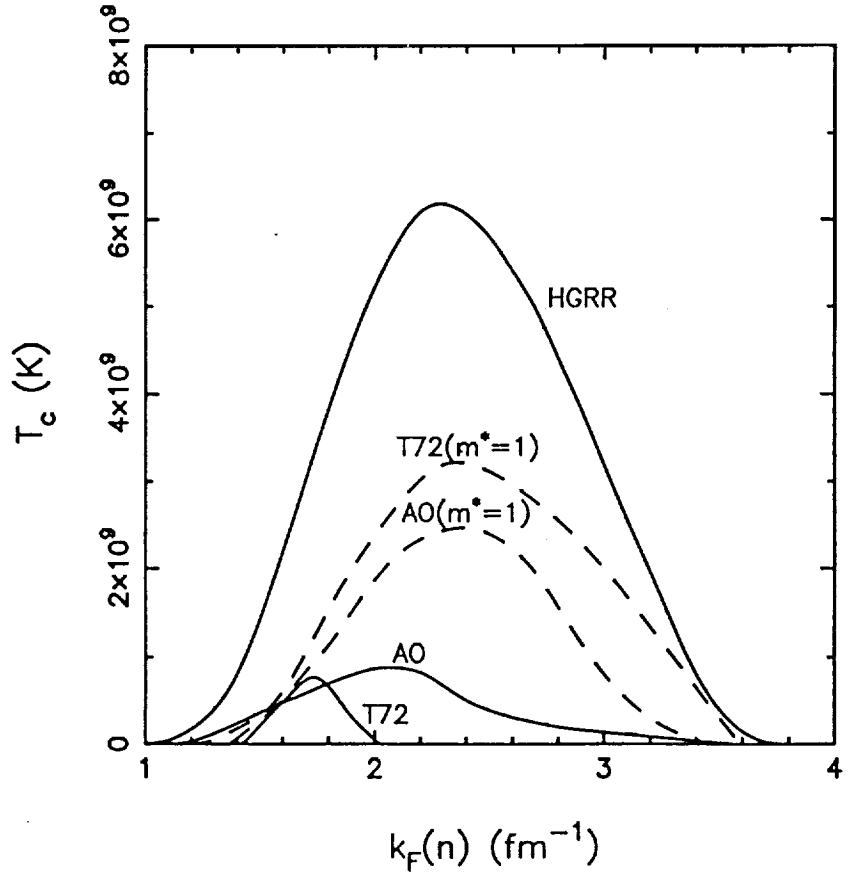
b) neutron $^3p_2$ pairing
T_c (K)
$k_F(n)$ (fm^{-1})
HGRR
T72(m*=1)
AO(m*=1)
AO
T72
0
2x10^9
4x10^9
6x10^9
8x10^9
1
2
3
4

Figure 1

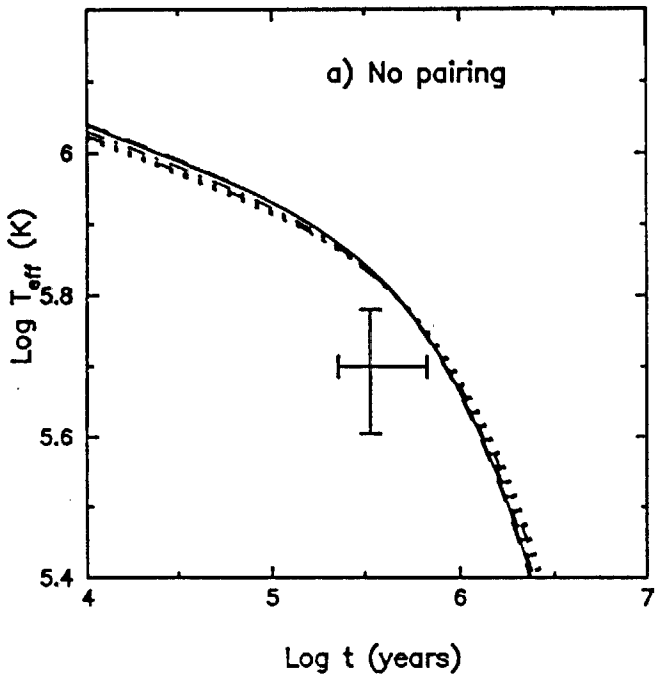
a) No pairing
Log T_{eff} (K)
Log t (years)
6
5.8
5.6
5.4
4
5
6
7

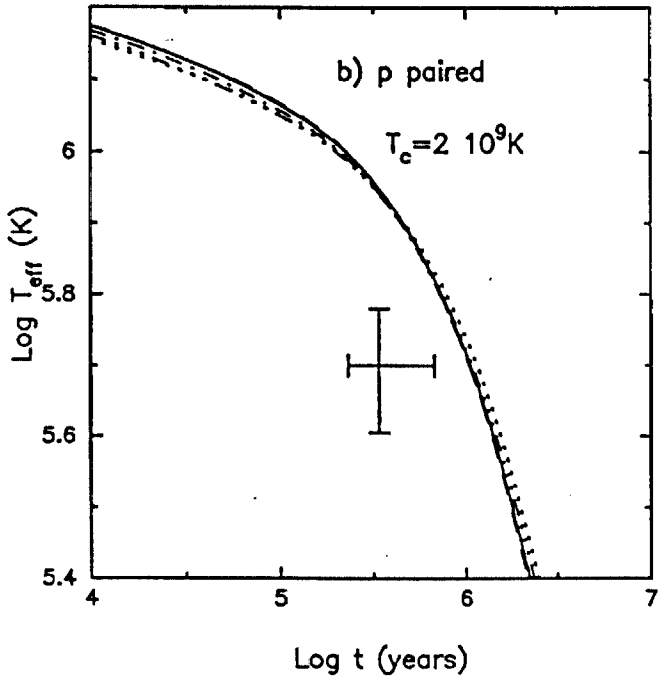
b) p paired
T_c=2 10^9K
Log T_{eff} (K)
Log t (years)
6
5.8
5.6
5.4
4
5
6
7

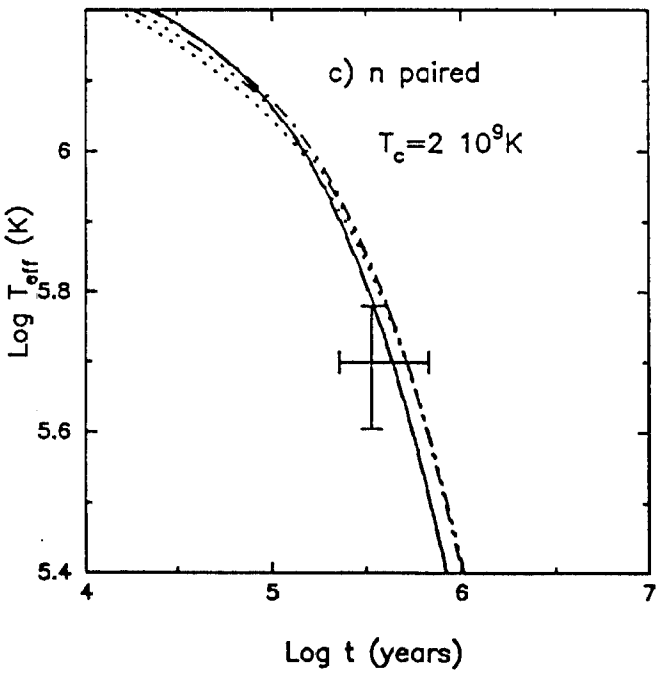
c) n paired
T_c=2 10^9K
Log T_{eff} (K)
Log t (years)
6
5.8
5.6
5.4
4
5
6
7

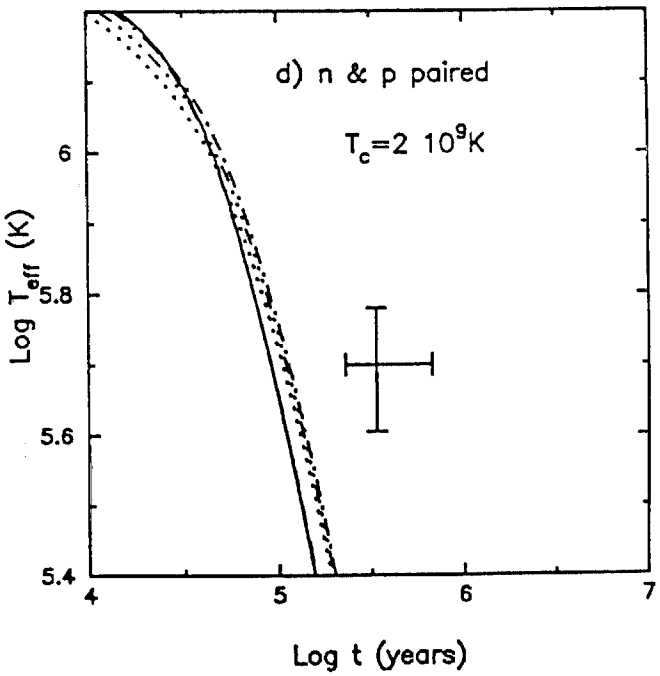
d) n & p paired
T_c=2 10^9K
Log T_{eff} (K)
Log t (years)
6
5.8
5.6
5.4
4
5
6
7

Figure 2

WFF (av14) Mass vs. Pairing

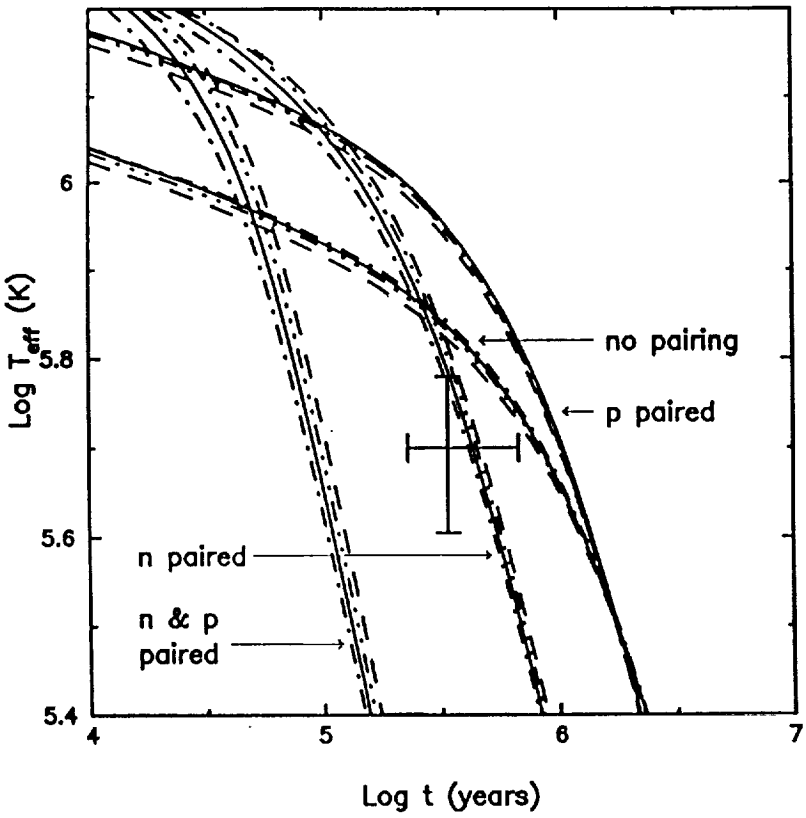

Figure 3

WFF (av14) : various neutron pairing

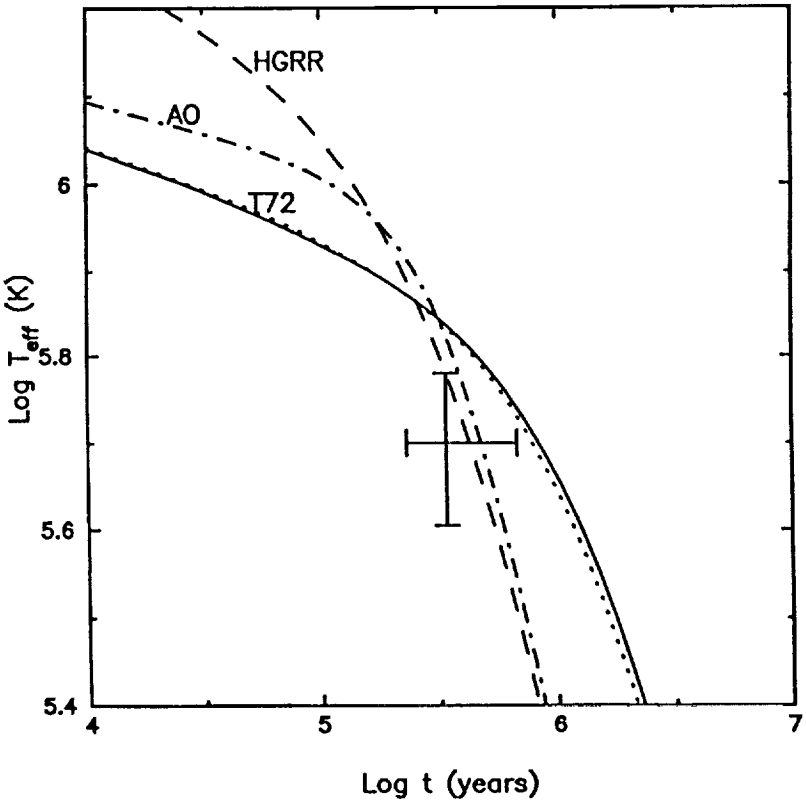

Figure 4

Cooling with/without kaons and core pairing